A novel framework for the assessment of hydro-meteorological risks taking into account nature-based solutions

ENVIRONMENTAL RESEARCH
LETTERS

LETTER • OPEN ACCESS

A novel framework for the assessment of hydro-meteorological risks taking into account nature-based solutions

To cite this article: L Brogno *et al* 2024 *Environ. Res. Lett.* **19** 074040

ENVIRONMENTAL RESEARCH
LETTERS

LETTER

A novel framework for the assessment of hydro-meteorological risks taking into account nature-based solutions

L Brogno*, F Barbano, L S Leo and S Di Sabatino

Physics and Astronomy Department, University of Bologna, Via Irnerio 46, Bologna, Italy
* Author to whom any correspondence should be addressed.

E-mail: luigi.brogno2@unibo.it

Keywords: hydro-meteorological hazards, risks, nature-based solutions, heatwaves, risk framework

Supplementary material for this article is available online

OPEN ACCESS

RECEIVED
31 January 2024

REVISED
23 May 2024

ACCEPTED FOR PUBLICATION
4 June 2024

PUBLISHED
21 June 2024

Abstract

The growing exposure to hydro-meteorological hazards translates into increasing risks for people, territories, and ecosystems. The frequency of occurrence and magnitude of these hazards are expected to further increase in the next decades urging tangible decisions to reduce anthropogenic climate change and adapt to the risks to be faced. In this context, risk assessment is an essential tool for becoming aware of dangers and taking countermeasures. This paper proposes a novel predictive, yet holistic, framework that allows to take into account multiple risks classified according to six research fields, i.e. healthcare, society, ecosystem, heritage, infrastructure, and agriculture. Each contribution to the overall risk is evaluated in terms of economic losses and carbon-dioxide emissions that in turn affect adaptation ability and contribute to exacerbating climate change. Both economic losses and emissions are estimated as a cost per day to support political decision-making processes. In this regard, the framework integrates the effects of adaptation and mitigation strategies to include societal capacities to cope with hazards and respond to their potential consequences. As a guideline, this study reports a preliminary investigation of a heatwave event over a portion of Bologna Province (Italy) concluding that the current use of air-conditioning systems is not sustainable leading to a huge amount of losses. The novel framework can be adopted in future studies for selecting more cost-effective strategies as expected for Nature-based Solutions (NbS). The framework can indeed stand as a tool for estimating the local impact of NbS in the current or future climate scenarios.

1. Introduction

Hydro-meteorological hazards consist of hazards resulting from atmospheric, hydrological, or oceanographic phenomena and processes (UNDRR 2017). These hazards include drought, erosion, floods, heatwaves, landslides, storm surges, and several others. Humans are contributing to the current growth of both magnitude and frequency of occurrence of these hazards (Masson-Delmotte *et al* 2021), especially for heatwaves (i.e. periods of abnormally hot and humid weather, IRDR 2014). These projections have aroused apprehension in decision-makers and the scientific community for the significant contribution to excess mortality and morbidity (Pörtner *et al* 2022). However, these risks are only the tip of the iceberg of all the risks undergone by people, ecosystems, livestock, crops, heritages, industries, and infrastructures when exposed to hazards, which occurrence may cause production losses, property damage, loss of livelihoods and services, or environmental degradation (UNDRR 2017). Risks may be realized only if hazard, exposure, and vulnerability are simultaneously not null as theorized by Crichton (1999) (i.e. Crichton's Risk Triangle) and assimilated by the Intergovernmental Panel on Climate Change (IPCC, Pörtner *et al* 2022). The hazard refers to the occurrence of events that may negatively affect people and the other exposed elements (i.e. the exposure) located where these events occur.

The vulnerability quantifies the susceptibility of these elements to be affected and includes the capacity to cope with the hazard through adaptation and mitigation strategies such as changes in people's behaviors, engineering solutions, and Nature-based Solutions (NbS). NbS are actions to protect, sustainably manage, and restore natural and modified ecosystems to address societal challenges effectively and adaptively, and provide both human well-being and biodiversity benefits (Cohen-Shacham *et al* 2016). Despite the increasing adoption of NbS worldwide (Debele *et al* 2023), a few frameworks have been developed in the context of NbS helping estimate risks arising from hydro-meteorological hazards (Shah *et al* 2020). For instance, Wei *et al* (2020) proposed an environmental-vulnerability framework in arid inland basins. Feng *et al* (2023) estimated the risk of hurricane-induced flooding by integrating both social and environmental indices of exposure, susceptibility, and lack of adaptive capacity. Holec *et al* (2021) added a vegetation layer to the hazard component for integrating the cooling effect of urban trees. However, risk assessment in the context of heatwaves is often limited to the human health at continental (e.g. Russo *et al* 2019, Yin *et al* 2020), national (e.g. Dubey *et al* 2021, Kc *et al* 2021) or city (e.g. Tomlinson *et al* 2011, Aubrecht and Özceylan 2013) scales for highlighting the most at-risk neighborhoods (e.g. Buscail *et al* 2012, Johnson *et al* 2016), estimating the heat-related mortality risk (e.g. Taylor *et al* 2015, Zemtsov *et al* 2020) or showing changes in return periods of mortality (e.g. Lüthi *et al* 2023). Most of these studies have reported maps in which the risk is dimensionless or presented in classes (e.g. from low to high risk) helping the comparison between areas but limiting the quantitative information of the output. A few papers have also addressed other risks such as the consumption of energy (Lee *et al* 2020) and economic losses resulting from the decrease in labor productivity (Stalhandske *et al* 2021).

The following paper aims to present a novel framework that quantifies risks resulting from hydro-meteorological hazards as a cost per day by integrating both climate and economic contributions into the IPCC's definition of risk. This pragmatic output allows us to compare contributions from different research fields, i.e. healthcare, society, ecosystem, heritage, infrastructure, and agriculture. The framework includes the concept of NbS as sustainable and cost-effective strategies. After this introductory section, the paper is structured as follows. Section 2 describes the novel framework to assess hydro-meteorological risks including the NbS contributions. Section 3 describes the methodology, data collection, and processing carried out for a preliminary application to a heatwave event. Section 4 shows the application results. Finally, section 5 draws the conclusions.

2. A novel risk framework for hydro-meteorological hazards

The increasing severity and frequency of hydro-meteorological hazards are raising the state of alert of the scientific community urging the development of novel risk frameworks that include adaptation and mitigation strategies. The current study proposes a predictive framework that assesses the economic losses and emissions of carbon dioxide (CO_2), incorporating the effects of strategies such as NbS. The framework adopts Crichton's Risk Triangle which theorizes that each risk (R) materializes only if hazard (H), exposure (E), and vulnerability (V) spatially and temporally coexist, i.e.

$$R = H \times E \times V. \quad (1)$$

Despite its apparent simplicity, the practical estimate is not straightforward because hydro-meteorological hazards can affect the exposed elements through a wide variety of potential impacts. To bypass this complexity, the risk is here decomposed into sub-risks classified according to six research fields, i.e. healthcare HC, society S, ecosystem EC, heritage HR, infrastructure I, and agriculture A (figure 1).

Since sub-risks can result in relevant economic losses and additional emissions of CO_2, sub-risks are classified in economic (subscript €) or climate (subscript CO_2) risk contributions. The framework includes climate sub-risks because emissions are the main driver of the current anthropogenic global-warming resulting in a higher frequency and magnitude of hot extremes, heavy precipitations, and drought (Masson-Delmotte *et al* 2021). All the contributions are measured as the daily loss of money required to cope with a hydro-meteorological event (i.e. a cost per day). This pragmatic choice allows the quantitative comparison of sub-risks that usually are evaluated with different measurement units. Climate sub-risks are expressed as a cost by using the equivalent price for a ton of emitted CO_2 (C_{CO_2}, Kikstra *et al* 2021) which is a climate measurement of the projected social cost taking into account long-term temperature growth feedback on economic trajectories, mean annual temperature anomalies, and permafrost-carbon and surface-albedo feedbacks. Other greenhouse gas emissions are converted into CO_2 equivalent. Economic and climate sub-risks also include the effects of adaptation/ mitigation strategies and the total cost spent for their implementation. In particular, the framework integrates contributions of NbS which are expected to reduce risks sustainably and cost-effectively (e.g. Sahani *et al* 2019). These contributions are considered as risks because NbS are themselves elements exposed to the hazard during their entire lifetime. The interaction between NbS and hydro-meteorological events is continuous and may

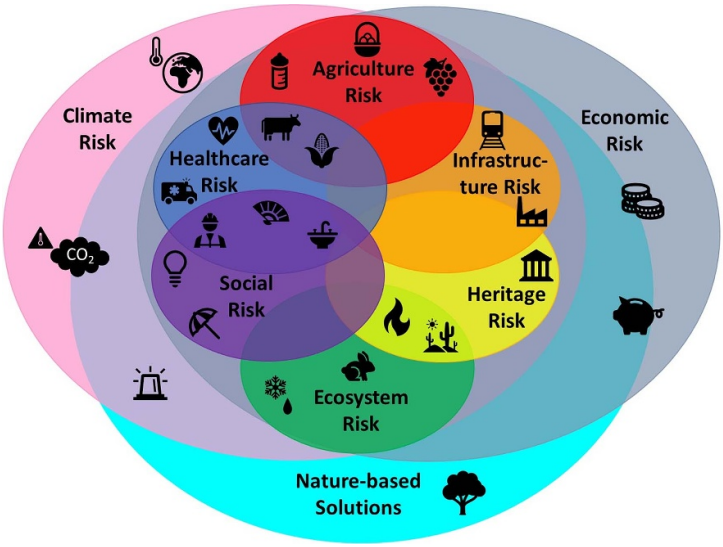

Figure 1. Conceptual scheme that summarizes the risks incurred by exposed elements when a hydro-meteorological event occurs. The scheme also includes the concept of NbS as adaptation and mitigation strategies that can reduce risks by addressing the hazardous event.

lead to extra measures of maintenance, enhancement, or restoration.

In the end, economic and climate sub-risks are summed in the economic ($R_€$) and climate (R_{CO_2}) risks. The total risk (R_T) is given by the summation of R_{CO_2} and $R_€$. The mathematical structure of this novel framework is summarized in figure 2. The following subsections will provide more details concerning the assessment of risk components and an overview of possible applications.

2.1. Assessment of hazard, exposure, and vulnerability

The novel framework follows the IPCC's definition of H, E, and V (Pörtner *et al* 2022). The quantity H is the potential occurrence of an event that may cause loss of life, health, property, infrastructure, livelihoods, service provision, ecosystems, and environmental resources. The framework requires quantifying H as the time-dependent magnitude of an event normalized according to its climatology. H depends on the event duration because their persistence or recurrence may lead to both acclimatization or stress exacerbation felt by the exposed elements. The quantity E is defined as the presence of people, livelihoods, species or ecosystems, environmental functions, services, resources, infrastructure, economic, social, and cultural assets in places and settings that could be adversely affected by the occurrence of hazardous events. Accordingly, E is a function of land-use and census data. The predisposition to be adversely affected is the vulnerability V, which encompasses a variety of concepts including susceptibility to harm and lack of capacity to cope and adapt. The quantity V is estimated in the framework as a cost per day per unit of exposed element by building distinct functions for each sub-risk as follows

$$V = F_V \times C, \tag{2}$$

where F_V is a vulnerability factor that links the exposed element to its predisposition to be affected or affect the environment during hazardous events, and C is the associated cost if the predisposition would result in damage. The predisposition is here estimated from the impacts experienced in previous events.

2.2. Assessment of NbS impacts

To include adaptation and mitigation strategies into the framework, we have decided to follow an ecosystem-service approach focusing on NbS as solutions that can reduce both the economic and climate risks during hydro-meteorological events (figure 1). NbS can locally modify the physical processes that regulate the hazard (H) and how the element exposed may be harmed (V). Moreover, NbS are green and blue elements included in E.

The cost-effectiveness of an NbS can be estimated at the local scale by defining the local impact of NbS (I_{NbS}) as

$$I_{NbS} = 100\left(\frac{\overline{(R_T)_b - (R_T)_a}\Big|_{localscale}}{(R_T)_b} - f_{cl}\right) \tag{3}$$

where the overbar denotes the time average during hydro-meteorological events that occur over climate scales, R_T is locally calculated before (subscript b) and after (subscript a) the NbS implementation, and f_{cl} is a climate factor evaluated at a larger area in which

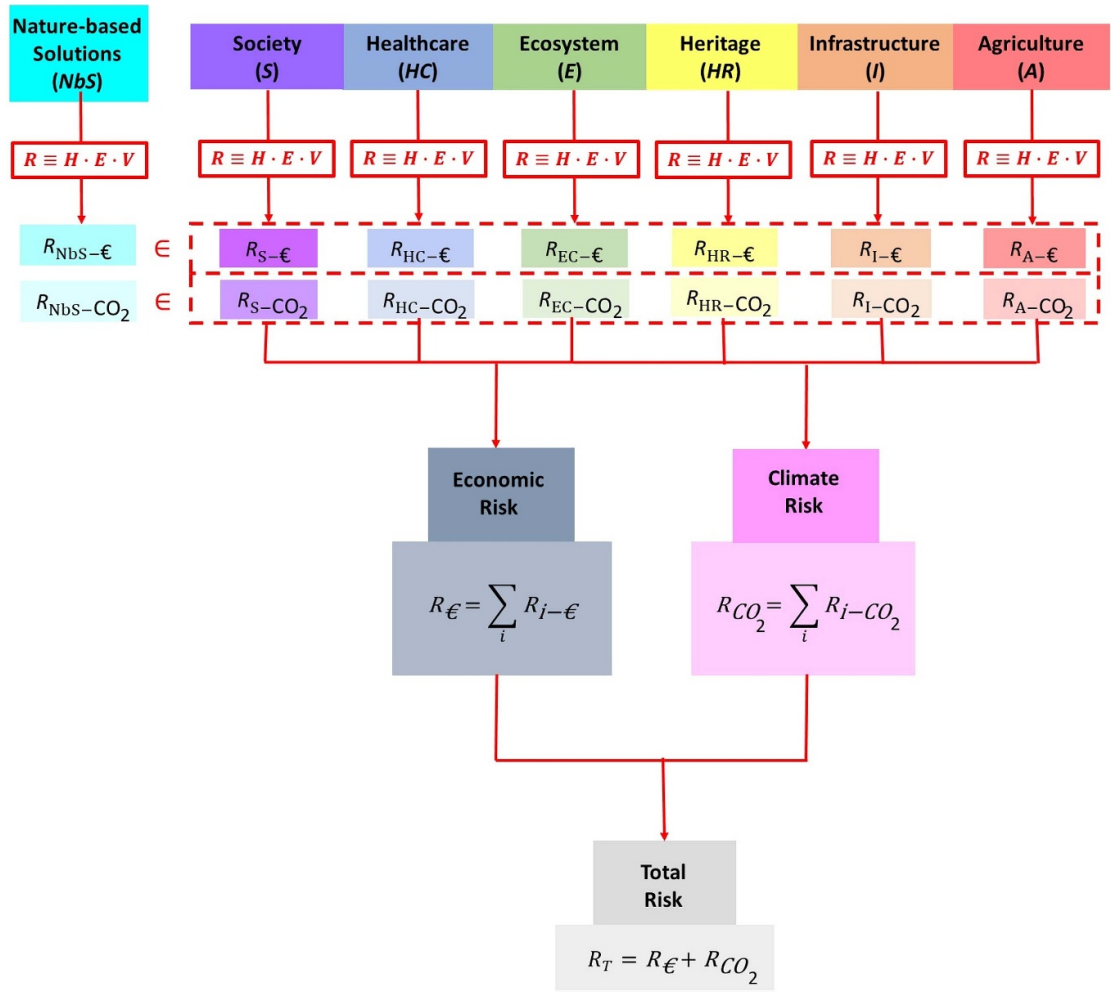

Figure 2. Mathematical structure of the novel risk framework in which the total risk R_T is given by the sum of the economic ($R_{€}$) and climate (R_{CO_2}) risks that may affect each ith research field, i.e. society (S), healthcare (HC), ecosystem (EC), agriculture (A), infrastructure (I), and heritage (HR). $R_{€}$ and R_{CO_2} also include the economic losses and CO_2 equivalent costs resulting from the entire lifetime of NbS and other adaptation/ mitigation strategies.

the NbS effectiveness is expected to be negligible. f_{cl} is computed as

$$f_{cl} = \overline{\left.\frac{(R_T)_b - (R_T)_a}{(R_T)_b}\right|_{\text{macroscale}}} \quad (4)$$

and introduced in I_{NbS} to subtract the contribution of large-scale climate variations to the local change over time of R_T.

2.3. Overview of framework applications

The adoption of a universally accepted definition of risk from IPCC (Pörtner *et al* 2022) allows assuming the framework can be adapted to all the hydro-meteorological hazards by integrating a broad range of sub-risks through only scientific-based indicators. Since the vulnerability factors are retrieved from past events, the estimated risks represent an average condition expected over several events rather than a prediction of the outcomes that will occur in a single event. The variability between events can be taken into account through sensitivity analyses, especially when the evolution of the hazard H is dominated by stochasticity such as wildfires that are affected by the fine-grained structure of burning. The framework can be used to both reanalyze past events and predict the potential risks in current and future climate scenarios. For instance, the framework can be adopted in early-warming systems by linking the estimates with case-dependent thresholds based on the local economy. The final estimate as a cost per day derives from the central role of the economic aspects in political decisions. The inclusion of climate sub-risks is essential because the lower the global-warming level is, the lower the magnitude and frequency of occurrence of hydro-meteorological hazards should be (Masson-Delmotte *et al* 2021). Following this evidence, the framework integrates the concept of NbS as strategies that may prevent economic losses by affecting CO_2 emissions and weather variables. However, the framework allows the introduction of vulnerability factors concerning other strategies such as air-conditioning systems. Since hydro-meteorological events are related to climate extremes and NbS are

expected to cope with these events during their entire life cycle, a comprehensive cost-effectiveness analysis requires data over years or tens of years. These time series can be obtained through modeling simulations of climate and socio-economic data that allow applying the framework over several synthetic events.

3. Preliminary application: methodology, data collection and processing

This section discusses the setup for an application example that serves as a guideline for future use. This application investigates a single day (i.e. 22 July 2022) of the heatwave event nicknamed Apocalypse4800 by Italian newspapers because the freezing level in Northern Italy had reached the top of Mont Blanc. The study area is bounded by the following ranges of latitude $lat \in [44.25 - 44.65]$ and longitude $long \in [11.15 - 11.55]$ allowing for the analysis over a significant portion of Bologna Province without trespassing in other ones. This portion includes 16 cells (CE) with each a resolution of $0.1° \times 0.1°$. Each *CE* will be identified by its row and column numbers (e.g. CE1–1 and CE4–4 are the top-left and bottom-right cells, respectively). Since NbS usually affect the risk on local scales (e.g. from the street to the city scale), this coarse resolution does not allow for the integration of the NbS concept. Table 1 reports the sources, spatial resolution, and temporal range of the data used in this application which is not comprehensive of the entire framework because, at least to our knowledge, several sub-risks cannot be currently estimated due to the unavailability of data or the lack of scientific research concerning the relationship between heat and vulnerability. The current application has selected the following sub-risks as representative of the exposed elements located in the study area during summer: 1) excess people mortality (in the healthcare risk R_{HC}), 2) the usage of air-conditioning systems (social risk R_S), 3) the compound occurrence of wildfires in woodlands (ecosystem risk R_{EC}), and 4) excess cattle mortality, the reduction in milk production and variations in the enteric-fermentation process (agricultural risk R_A).

3.1. Hazard

Heatwaves have been identified as 3 or more consecutive days with a daily maximum temperature (T_{max}) above the 90th percentile evaluated over the last 30 years centered on a 31-day window (Russo *et al* 2014, 2015). This definition has been chosen for its climate perspective and generality that allows the detection of heatwaves worldwide. A suitable data set has been extracted from ERA5-Land reanalysis (Muñoz Sabater 2019). This data set includes hourly 2-m air temperature T (K), dew point T_{dew} (K) and relative humidity RH (%) calculated following the formula reported by Alduchov and Eskridge (1996):

$$\mathrm{RH} = 100\exp\left[\frac{17.625\,(T_{\mathrm{dew}} - 273.15)}{T_{\mathrm{dew}} - 30.11}\right] \times \left\{\exp\left[\frac{17.625\,(T - 273.15)}{T - 30.11}\right]\right\}^{-1}. \quad (5)$$

After the heatwave identification, a representative variable x has been selected for each exposed element to link heatwaves with their vulnerability. Since both T and RH affect the thermal comfort of living beings, x was the daily maximum heat index for people (HI, Guarino *et al* 2014) and temperature humidity index for cattle (THI, Lallo *et al* 2018). The daily T_{max} has been selected for the risk of wildfires in woodlands. Then, H has been estimated through a slightly modified version of the daily magnitude M_d (Russo *et al* 2014, 2015), i.e.

$$M_{\mathrm{d}} = \frac{x - x_{25}}{x_{75} - x_{25}}, \quad (6)$$

where x_{75} and x_{25} are respectively the 75th and 25th percentiles of x evaluated over 30 years centered on a 31-day window. These percentiles were not calculated by using the annual x over 30 years as in the original definition because the adoption of the framework would have been limited only to summer months. Using the 31-day window, the warm spells can be captured; this has implications in agriculture when unseasonably warm weather occurs during the reproductive phases of crops.

Except for the risks that result from compound hazards (e.g. wildfires), the acclimatization index for the excess heat EHI (accl) (Nairn and Fawcett 2015) has been introduced when the exposed elements are living beings. EHI (accl) has been estimated for the jth day by comparing x in the last 3 days with the previous 30 days, i.e.

$$\mathrm{EHI\ (accl)} = \frac{x_j + x_{j-1} + x_{j-2}}{3} - \frac{x_{j-3} + x_{j-4} + \ldots + x_{j-32}}{30}. \quad (7)$$

Then, the H component has been computed by combining (6) and (7) as follows

$$H = \begin{cases} \dfrac{M_{\mathrm{d}} \times \max[1,\mathrm{EHI(accl)}]}{\mathrm{median}(M_{\mathrm{d}} \times \max[1,\mathrm{EHI(accl)}])} & \text{for living beings} \\ \dfrac{M_{\mathrm{d}}}{\mathrm{median}(M_{\mathrm{d}})} & \text{otherwise} \end{cases} \quad (8)$$

in which H is normalized by the median value across all the heatwave events that occurred in the previous 10 years. A 10-year threshold has been selected instead of a 30-year one for enhancing the applicability of H computation. Since identifying heatwave events required a 30-year climatology, calculating the median across the events in the previous 30 years would require data for the previous 60 years. However, a 10-year threshold can preserve the climate signal (i.e. requiring data for the previous 40 years) and provide a significant number of events, especially

Table 1. References, spatial scale, and temporal range for each data used to estimate the hazard H, exposure E, and vulnerability V components. V terms are further classified in economic (€) or climate (CO_2) contributions related to the six research fields, namely, society S, healthcare HC, ecosystem EC, agriculture A, infrastructure I, and heritage HR.

Variables	Component	Values	References	Spatial Scale	Temporal Range
2-m air temperature T	H		Muñoz Sabater (2019)	$0.1° \times 0.1°$	1981–2022
2-m dew point T_{dew}	H		Muñoz Sabater (2019)	$0.1° \times 0.1°$	1981–2022
Land use	E		ERR (2020)	2.00×10^{-1} m	2017
Total human population: a) every age group b) elderly	E	 a) 7.18×10^5 people b) 1.77×10^5 people	ISTAT (2022b)	Municipal	2022
Premature-death rate PD	$V_{HC-€}$	9.18×10^{-7} d^{-1}	OECD (2019)	National	Averaged between 2010 and 2019
Cost of a life lost C_L	$V_{HC-€}$	3.00×10^6 € people^{-1}	OECD (2019)	National	2019
Air-conditioning usage U_{AC}	$V_{S-€}$, V_{S-CO_2}	6.28 h d^{-1} people^{-1}	ISTAT (2021)	National	2021
People with air-conditioners at home P_{AC}	$V_{S-€}$, V_{S-CO_2}	6.03×10^{-1}	ISTAT (2021)	Regional	2021
Direct cost for air conditioning C_{AC}	$V_{S-€}$	3.1×10^{-1} € h^{-1}	ARERA (2022)	National	Summer 2022
CO_2 emission for electricity Production EM_{kWh}	V_{S-CO_2}	4.37×10^{-4} ton h^{-1}	ISPRA (2023)	National	Projected to 2022
Cost of CO_2 emissions C_{CO_2}	V_{S-CO_2}, V_{A-CO_2}, V_{EC-CO_2}	3.07×10^2 $ ton^{-1}	Kikstra *et al* (2021)	—	Simulated between 2020 and 2300
Exchange rate dollars-euros ER_C	V_{S-CO_2}, V_{A-CO_2}, V_{EC-CO_2}	9.80×10^{-1} € $^{-1}$	X-Rates (2023)	—	July 2022
Cost for air-conditioning CO_2 emissions EM_{AC}	V_{S-CO_2}	1.2×10^{-1} € h^{-1}	equation (12)	—	—
Total cattle population: a) every cattle b) adult cattle c) adult dairy cattle	E	 a) 3.33×10^4 cattle b) 1.76×10^4 cattle c) 1.38×10^4 cattle	IHM (2022) EER (2010)	Regional Provincial	2010–2022 2010
Cattle market value MV_c	$V_{A-€}$	2.00×10^3 € cattle^{-1}	In line with prices reported by ISMEA (2022)	National	2022
Milk market value MV_m	$V_{A-€}$	7.00×10^{-1} € kg^{-1}	CLAL (2022b)	Regional	2022
Cattle premature-death Rate PD_c	$V_{A-€}$	9.00×10^{-6} d^{-1}	Vitali *et al* (2015)	National	Averaged between 2002 and 2007
Milk production P_m	$V_{A-€}$	2.43×10^1 kg d^{-1} cattle^{-1}	CLAL (2022a)	National	2022
Reduction in milk production RE_m	$V_{A-€}$	$(2.16 - 2.70) \times 10^{-1}$	equation (15)	—	—
Cattle CH_4 emissions EM_{CH_4}	V_{A-CO_2}	1.80×10^{-4} ton d^{-1} cattle^{-1}	Yadav *et al* (2016)	—	—

(Continued.)

Table 1. (Continued.)

Variation in cattle CH_4 emissions VT_{CH_4}	V_{A-CO_2}	1.26×10^{-1}	Yadav *et al* (2016)	—	—
CH_4 global warming potential GWP_{CH4}	V_{A-CO_2}	27.2	Masson-Delmotte *et al* (2021)	—	—
Total woodland extension	E	2.77×10^4 ha	ERR (2020)	2.00×10^{-1}	2017
Seasonal fire Weather index FWI_s	$V_{EC-€}$, V_{EC-CO_2}	9.0	Copernicus Climate Change Service (2020)	Provincial	Simulated between 2021 and 2040
Forecasted fire Weather index FWI_{fc}	$V_{EC-€}$, V_{EC-CO_2}	43.4 – 56.4	GWIS (2023)	8.00×10^3 *m*	22 June 2022
Woodland burnt area BA	$V_{EC-€}$, V_{EC-CO_2}	2.10×10^{-6} d^{-1}	CFPC (2021) CFPC (2019)	Regional	2021 2017–2019
Wildfire cost C_{wf}	$V_{EC-€}$	1.02×10^4 € ha^{-1}	IQ FireWatch (2023), confirmed by Italian Confederation of Direct Farmers	—	—
Wildfire emissions EM_{wf}	V_{EC-CO_2}	30.2 ton ha^{-1}	Copernicus Climate Change Service (2022)	National	2022

in current and future climate scenarios in which heatwaves are becoming more frequent worldwide.

3.2. Exposure

The study area includes a multitude of facets in terms of land use and altitude as shown by figure 3. The Northern part is a portion of Po Valley in which the main land use is croplands. The hills and mountains of Tuscan–Emilian Apennines extend south of Bologna which is located in CE2–2 and CE2–3. Apennines are rich in woodlands surrounded by croplands in the inland valleys. The hectares covered by each land use have been calculated by counting the number of pixels with the same RGB color triplet. This calculation has enabled us to estimate the woodland hectares. Since most of the livestock in Po Valley lives in intensive animal farming, cattle were proportionally distributed over cells by considering the hectares covered by agro-zootecnical areas. This application has considered only adults over 24 months old for excess mortality, adult dairy cattle that have given birth for milk production, and every cattle for changes in enteric fermentation. The last selected exposed elements are elderly over 64 years old for excess mortality and the entire population for the use of air-conditioning systems. The population has been estimated by summing demographic data concerning municipalities located inside each cell. Despite croplands being the main land use, crop losses have not been considered in this summer application because the main crops are wheat and spelt produced during wintertime (ISTAT 2022a).

3.3. Vulnerability

Vulnerability (V) has been estimated as a cost per day per unit of exposed element according to (2). Excess mortality has been included in the economic vulnerabilities for the healthcare system ($V_{HC-€}$) as follows

$$V_{HC-€} = PD \times C_L, \tag{9}$$

where PD is the premature-death rate for elderly exposed to high temperatures, and C_L is the cost of a life lost assuming this value is equal to the value of a statistical life VSL which is a statistical index (Adélaï de *et al* 2022) that estimates the average economic amount the population is willing to pay for a reduction of mortality equal to one person over 1×10^5.

A widespread strategy for reducing mortality is the adoption of air-conditioning systems (e.g. Nunes *et al* 2011). However, air conditioning increases both energy consumption and CO_2 emissions contributing to the economic $V_{S-€}$ and climate V_{S-CO_2} social vulnerabilities. Losses have been estimated as

$$V_{S-€} = U_{AC} \times P_{AC} \times C_{AC}, \tag{10}$$

$$V_{S-CO_2} = U_{AC} \times P_{AC} \times EM_{AC}, \tag{11}$$

where U_{AC} is the daily average use, P_{AC} is the fraction of people with air conditioning at home, C_{AC} is

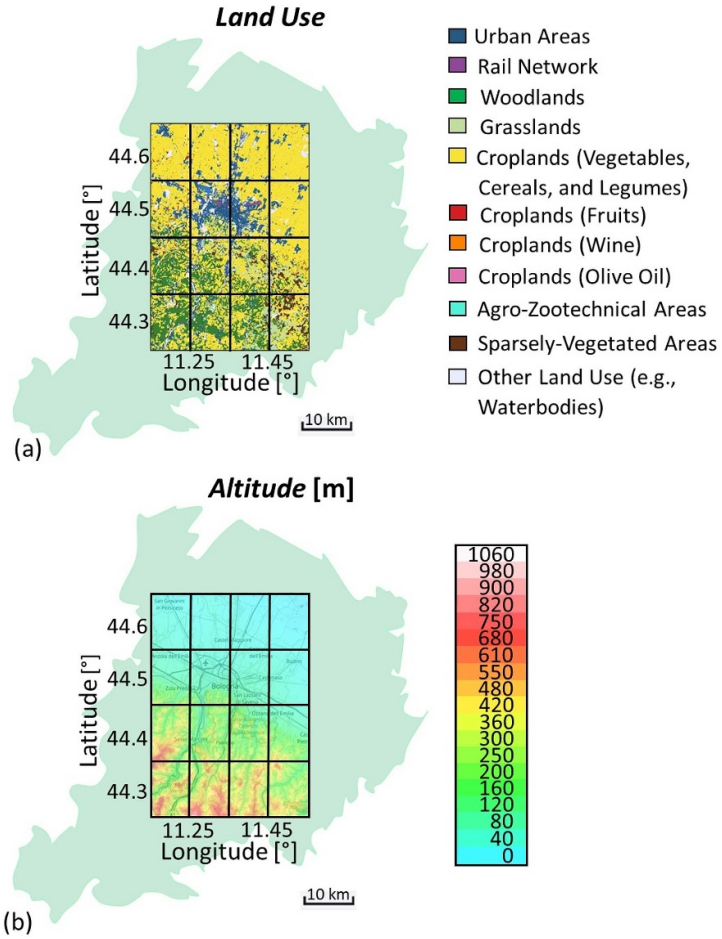

Figure 3. Land use (a, ERR 2020) and altitude (b) maps for the study area in Bologna Province. Altitude map is available on the website https://it-it.topographic-map.com/map-h28dn/Bologna/ and has been produced in OpenStreetMap through the digital elevation model TessaDEM. (a) Adapted from [https://geoportale.regione.emilia-romagna.it/catalogo/dati-cartografici/pianificazione-e-catasto/uso-del-suolo/layer-9]. CC BY 3.0. (b) Adapted from [https://it-it.topographic-map.com/]. © IOP Publishing Ltd CC BY-NC-SA 3.0.

the hourly average cost supposing these systems consume 1 kWh, and $\mathrm{EM_{AC}}$ is the hourly average equivalent cost for CO_2 emissions. $\mathrm{EM_{AC}}$ has been estimated as follows

$$\mathrm{EM_{AC}} = \mathrm{EM_{kWh}} \times C_{\mathrm{CO_2}} \times \mathrm{ER_C}, \tag{12}$$

where $\mathrm{EM_{kWh}}$ is the hourly CO_2 emission for the production of 1 kWh, $C_{\mathrm{CO_2}}$ is the equivalent price for a ton of emitted CO_2, and $\mathrm{ER_C}$ is the average exchange rate between dollars and euros.

If strategies are not adopted in intensive farming, cattle can be affected by heat stress leading to the following economic $V_{\mathrm{A-€}}$ and climate $V_{\mathrm{A-CO_2}}$ agricultural vulnerabilities:

$$\begin{aligned} V_{\mathrm{A-€}} &= V_{\mathrm{em_c}} + V_{\mathrm{m}} \\ &= \mathrm{MV_c} \times \mathrm{PD_c} + \mathrm{MV_m} \times P_{\mathrm{m}} \times \mathrm{RE_m}, \end{aligned} \tag{13}$$

$$\begin{aligned} V_{\mathrm{A-CO_2}} &= \mathrm{EM_{CH_4}} \times \mathrm{VT_{CH_4}} \times \mathrm{GWP_{CH_4}} \\ &\quad \times C_{\mathrm{CO_2}} \times \mathrm{ER_C}, \end{aligned} \tag{14}$$

where $V_{\mathrm{em_c}}$ and V_{m} are the contributions of cattle excess mortality and milk-production losses, respectively. $\mathrm{MV_c}$ and $\mathrm{MV_m}$ are the average market values of a cattle and a kilogram of milk for the production of Parmigiano Reggiano, respectively. This milk price has been selected because 82% of Italian milk is intended for cheese production and Parmigiano Reggiano is a locally valued product. $\mathrm{PD_c}$ is the daily premature-death rate for cattle during heatwaves in July, P_{m} is the average daily production of milk from a single cattle, $\mathrm{EM_{CH_4}}$ is the average methane production in the temperature range $T \in [298 - 303]\ K$, $\mathrm{VT_{CH_4}}$ is the average variation in methane production when the temperature rises at $T \in [308 - 313]\ K$, $\mathrm{GWP_{CH_4}}$ is the global warming potential of methane over 100 years, and $\mathrm{RE_m}$ is the average reduction in milk production during heatwaves. A dimensionless version of the formula proposed by Berry *et al* (1964) has been adopted for $\mathrm{RE_m}$:

$$\mathrm{RE_m} = \frac{0.024\,74 \times P_{\mathrm{m}} \times \mathrm{THI} - 1.736 \times P_{\mathrm{m}} - 1.075}{P_{\mathrm{m}}}. \tag{15}$$

Wildlife is exposed to heatwaves as well, such as when wildfires occur in woodlands due to the increasingly drier soil. Wildfire occurrence leads to both the loss of ecosystems and additional CO_2 emissions ($V_{EC-€}$ and V_{EC-CO_2}, respectively) that have been estimated as

$$V_{EC-€} = \frac{FWI_{fc}}{FWI_s} \times BA \times C_{wf}, \quad (16)$$

$$V_{EC-CO_2} = \frac{FWI_{fc}}{FWI_s} \times BA \times EM_{wf} \times C_{CO_2} \times ER_C, \quad (17)$$

where BA is the average regional daily fraction of burnt area in woodlands during the wildfire season (June–September). FWI_{fc} and FWI_s are the daily-forecasted and seasonal fire weather index, respectively. FWI estimates the likelihood of occurrence of wildfires based on fuel moisture and weather (Van Wagner *et al* 1985). The values of FWI_{fc} for 22 June 2022 correspond to very high and extreme danger conditions. C_{wf} and EM_{wf} are the average cost and CO_2 emission per burnt hectare, respectively. C_{wf} includes the economic losses related to firefighting, damage, clean-up, and subsequent reforestation.

3.4. Risk

The overall risk for each research field has been estimated by applying Crichton's Risk Triangle as follows:

$$R_{HC} = R_{HC-€} = H(HI) \times E[\text{elderly}] \times V_{HC-€}, \quad (18)$$

$$R_S = R_{S-€} + R_{S-CO_2} = H(HI) \times E[\text{people}] \times \left(V_{S-€} + V_{S-CO_2}\right), \quad (19)$$

$$R_A = R_{A-€} + R_{A-CO_2} \quad (20)$$

$$= H(THI) \times E[\text{cattle}] \times \left(V_{A-€} + V_{A-CO_2}\right), \quad (21)$$

$$R_{EC} = R_{EC-€} + R_{EC-CO_2} \quad (22)$$

$$= H(T) \times E[\text{woodlands, ha}] \times \left(V_{EC-€} + V_{EC-CO_2}\right). \quad (23)$$

According to their classification as climate or economic contributions, the sub-risks of each field i are summed to obtain $R_€$ and R_{CO_2}:

$$R_€ = \sum_i R_{i-€}, \quad (24)$$

$$R_{CO_2} = \sum_i R_{i-CO_2}, \quad (25)$$

which are finally summed together to obtain the total risk

$$R_T = R_€ + R_{CO_2}. \quad (26)$$

The estimate of each risk as a cost per day is obtained by the product of E (i.e. the amount of each element) and V (i.e. a cost per day per unit of these elements). H is normalized to integrate the magnitude of an event compared to the climatology. For heatwaves, H acts as a temperature weight which is higher (lower) than 1 when the analyzed heatwave is more (less) intense than the median.

3.5. Data approximations

The framework requires the integration of several data whose spatial scales and temporal ranges may not coincide (table 1). The recommendation is to adopt local 1) socio-economic data (e.g. censuses, production rates, costs) referring to the same period as the hazardous event, and 2) data concerning the predisposition to be affected (e.g. rates of death, degradation, or occurrence of compound events) estimated from the impacts experienced in previous events. However, the lack of local data can often lead to the adoption of regional and national ones that depict the local conditions at a first approximation. Also, socio-economic data may not be updated to the year of interest. When these data are not available, data from multiple previous years can be averaged and their annual variability used as a metric of consistency. We suggest using data from the most recent year when the available years are few and scattered. An exception in the proposed application was the estimate of cattle population that was derived from both provincial data retrieved in 2010 and the most recent regional ones. In this particular case, the 2010 Bolognese population has been projected to 2022 proportionally to the regional increment.

Estimating daily V terms has required greater efforts because several data are provided for the entire summer or year. The original data has been divided for the number of days when the largest contribution to these data took place. For instance, a daily value for burnt area BA has been derived from an annual one by assuming wildfires spread only during wildfire season (June–September) as supported by (Copernicus Climate Change Service 2022). Instead, the premature-death rate PD has been obtained by assuming excess mortality is only induced by summer heatwaves because temperature and mortality are usually related by U- or V-shaped dose-response relationships (Gasparrini and Armstrong 2011). Finally, some original values have been divided by the number of elements located at the spatial scale to which data refer. For instance, daily milk production P_m has been derived from the national 2022 production divided by both 365 days and the number of Italian dairy cattle that have given birth (IHM 2022).

By carefully addressing the limitations associated to the temporal and spatial scales, it is possible to achieve an acceptable estimate of the sub-risks. As previously commented, the methodology need to be complemented by an analysis of uncertainties if the available data allowed to do that. This is out of

the scope of the current investigation since several data are provided without the associated uncertainties, requiring additional hypotheses for a sensitivity analysis.

4. Results

4.1. Hazard, exposure and vulnerability

The estimate of the total risk requires the setting up of H, E, and V maps for each sub-risk. H is estimated according to (8) and illustrated in figure 4 for people (a), cattle (b), and woodland wildfires (c). H is modulated according to the selection of proper variables able to describe the heat stress felt by each exposed element and the adoption of the acclimatization index for living beings (except for compound hazards).

The significant magnitude of the selected heatwave day has been confirmed by $H(T) \in [1.21 - 1.32]$ resulting in higher temperatures than the median over the previous 10 years. The adoption of variables that integrate both RH and acclimatization changes the cells in which the maximum values are reached. During the analyzed day, $H(\mathrm{HI}) \in [1.16 - 1.59]$ which is higher than $H(T)$ in the flat areas and lower in the mountainous ones. Instead, $H(\mathrm{THI}) \in [0.81 - 0.98]$ is lower than $H(\mathrm{HI})$ due to the different dependence on RH. Cattle are more sensitive to RH than humans because these animals have a less efficient sweating system. Since the selected heatwave day was less wet than the previous month, daily variations in THI are flattened and the cattle result more acclimatized than humans. These exposed elements are differently spread in the cells as shown by figure 5 for people (a), elderly (b), cattle (c), and woodlands (d). 64% of both total population and elderly live in the city of Bologna and its peri-urban areas located in CE2–2 and CE2–3. The other cells are not very inhabited, especially the mountainous ones. However, these cells are rich in woods up to 17% in CE4–1 and 15% in CE3–1. On the other hand, cattle are more widely distributed reaching the maxima in opposite cells (i.e. the 14% in CE1–1 and 9% in CE4–4, respectively).

A few V components are estimated in dependence on both T and RH. Figure 6 includes the economic ($V_{\mathrm{EN}-€}$, a) and climate ($V_{\mathrm{EN}-\mathrm{CO_2}}$, b) vulnerabilities related to ecosystems, and milk-production losses (contribution to the agriculture sub-risk $V_{\mathrm{A}-€}$, c) that result from a reduction in milk production ranged from 22% to 27%.

4.2. Risk

The integration of the H, E, and V maps leads to the assessment of risks R. Several papers report that a correlation between the adoption of air-conditioning systems and mortality reduction during heatwaves exists (e.g. Curriero *et al* 2002, Nunes *et al* 2011). Figure 7 shows the maps of the economic contribution to the healthcare risk $R_{\mathrm{HC}-€}$ (a) and social risk $R_{\mathrm{S}-€}$ (b), the climate contribution to the social risk $R_{\mathrm{S}-\mathrm{CO_2}}$ (c), and the overall social risk $R_{\mathrm{S}} = R_{\mathrm{S}-€} + R_{\mathrm{S}-\mathrm{CO_2}}$ (d). Despite the losses associated with excess mortality could be higher without the adoption of air conditioning, this adaptation strategy is not cost-effective in the current analysis. The sum of the potential losses in the urban cells (i.e. CE2–2 and CE2–3) are relevant reaching $R_{\mathrm{HC}-€} = 4.64 \times 10^5$ € d^{-1} and $R_{\mathrm{S}} = 1.14 \times 10^6$ € d^{-1}. Direct economic losses contribute to the 71% of R_{S}, while the remaining 29% derives from CO_2 emissions. The overall risk arising from the agricultural sector is three orders of magnitude lower than R_{S} as shown by figure 8 that includes the economic contributions $R_{\mathrm{A}-€}$ (a, cattle excess mortality; b, milk production), the negative climate contribution $R_{\mathrm{A}-\mathrm{CO_2}}$ (c, enteric fermentation), and the overall risk $R_{\mathrm{A}} = R_{\mathrm{A}-€} + R_{\mathrm{A}-\mathrm{CO_2}}$ (d). The maps of these risks follow the spatial distribution of E with higher values in CE1–1. The major economic risk is driven by the reduction in milk production that contributes to losses up to 8.62×10^3 € d^{-1} in this cell. Excess cattle mortality is instead totally exceeded by the negative contribution resulting from enteric fermentation. This climate term reduces R_{A} to 7.89×10^3 € d^{-1}. Lower estimates are obtained for the ecosystem risk resulting from wildfires in woodland hectares as shown in figure 9 that includes the economic $R_{\mathrm{EC}-€}$ (a), climate $R_{\mathrm{EC}-\mathrm{CO_2}}$ (b), and the overall risk $R_{\mathrm{EC}} = R_{\mathrm{EC}-€} + R_{\mathrm{EC}-\mathrm{CO_2}}$ (c). Despite the spatial distribution follows E with higher values in mountainous areas, the maxima are displaced in CE4–3 instead of CE4–1 due to the worse daily-forecasted WFI (49.2 and 43.4, respectively). R_{EC} is 1.19×10^3 € d^{-1} in CE4–3 whose main contributor is $R_{\mathrm{EC}-€}$ (the 53%).

Figure 10 shows the maps of the overall economic $R_{€}$ (a) and climate $R_{\mathrm{CO_2}}$ (b) risks, and the total risk $R_{\mathrm{T}} = R_{€} + R_{\mathrm{CO_2}}$ (c). R_{T} in the entire selected area is equal to 2.55×10^6 € d^{-1} resulting from $R_{€}$ (the 79%) and $R_{\mathrm{CO_2}}$ (the 21%). Since $R_{\mathrm{HC}-€}$ and R_{S} are the larger contributor to the huge amount of losses estimated in a single day for the selected portion of Bologna Province (the 69% and 28% of R_{T}, respectively), most of the losses may affect the city of Bologna (the 63%). However, this application also reveals that the sum of minor sub-risks such as $R_{\mathrm{CO_2}}$ can assume high absolute values (i.e. hundreds of thousands of euros in a single day), and some sub-risks may be locally non-negligible such as R_{A} in CE4–4 (the 68%).

5. Conclusions

This paper proposed a novel framework for the assessment of hydro-meteorological risks starting from the definition adopted by IPCC, i.e. the risk is given by the spatial and temporal overlaps of hazard, exposure, and vulnerability. This definition is used to estimate several economic and climate sub-risks

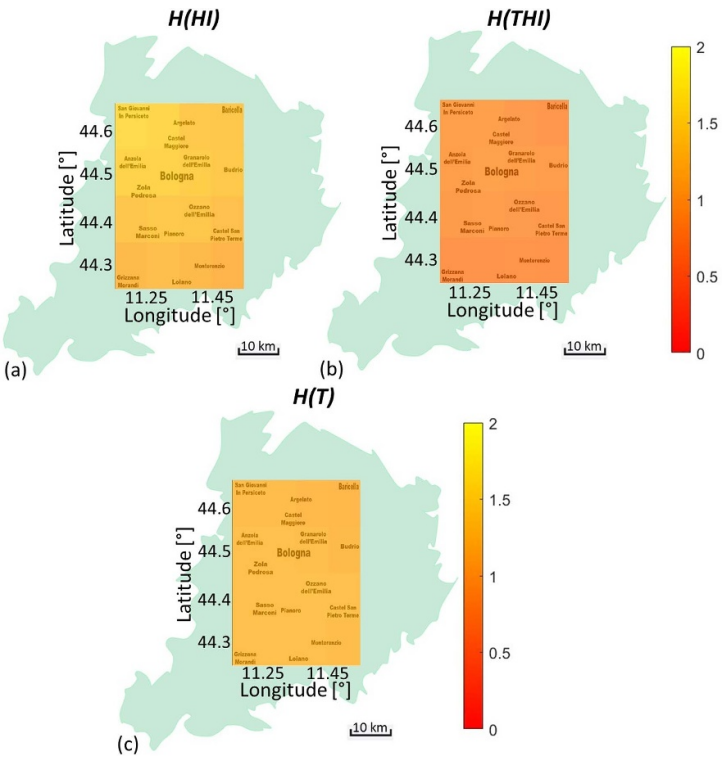

Figure 4. Hazard component H estimated from the heat index (HI) for people and elderly (a), the temperature humidity index (THI) for cattle (b), and temperature (T) for woodlands (c).

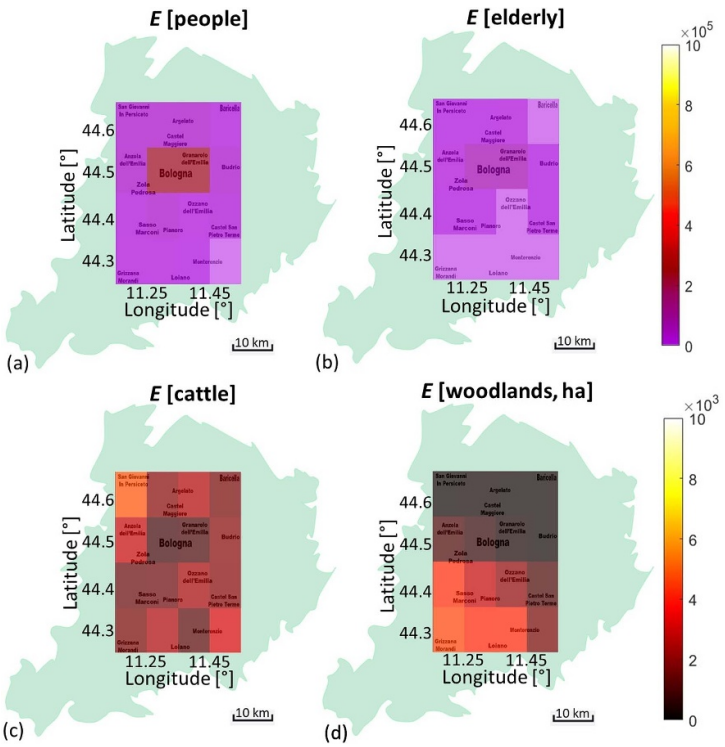

Figure 5. Exposure component E for people (a), elderly (b), cattle (c), and woodlands (d).

resulting from the occurrence of a hazardous event. These sub-risks include the contribution of mitigation and adaptation strategies such as NbS in reducing risks by locally affecting weather variables and CO_2 emissions. Since NbS are expected to be cost-effective, we have defined the local impact of NbS (I_{NbS}, equation (3)) as a tool to estimate the cost-effectiveness of NbS by comparing the total risk

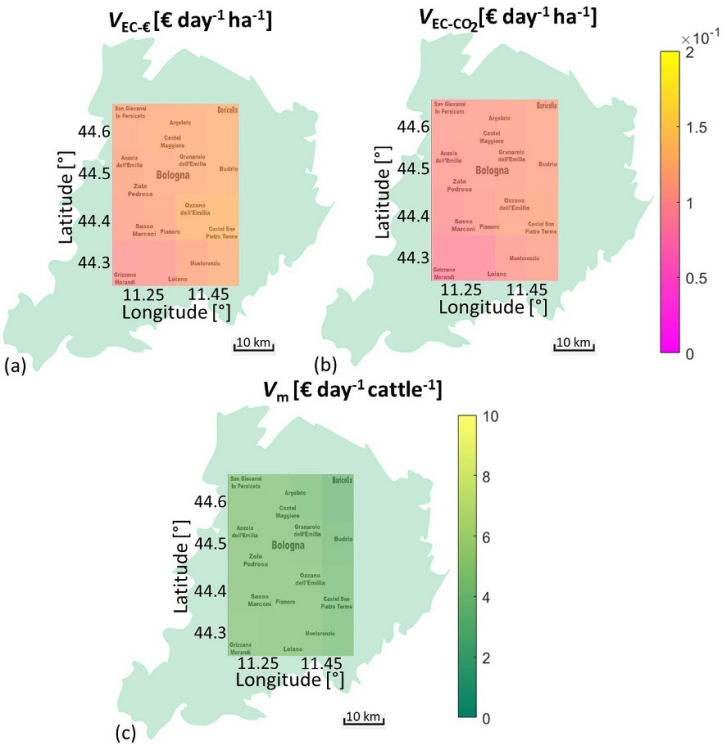

Figure 6. Vulnerability component V concerning the economic (a) and climate (b) contributions of woodland wildfires to the ecosystem sub-risk (i.e. $V_{EN-€}$ and V_{EN-CO_2}, respectively), and milk-production losses V_m (c) as part of the economic contribution of the agricultural sub-risk $V_{A-€}$.

before and after the implementation. This total risk is obtained as a cost per day by summing all the economic and climate sub-risks classified according to six research fields, i.e. healthcare, society, ecosystem, heritage, infrastructure, and agriculture. A cost per day is a pragmatic output that can help the decision-making process both in the current climate (e.g. by adopting the framework in early-warming systems) and in future one (e.g. by coupling the framework with socio-economic and climate projections).

The application of the developed risk framework, though simplified, serves the purpose of being a guideline for future studies. This application consists of a 1-day reanalysis of a significant heatwave event that involved Bologna Province (Northern Italy) in July 2022. The selected area (i.e. lat $\in [44.25 - 44.65]$, long $\in [11.15 - 11.55]$) includes several ecosystems such as the city of Bologna, croplands in the flat areas and woodlands in the mountainous ones. A few sub-risks have been estimated to represent the most valuable elements exposed to the analyzed summer heatwave. These sub-risks include human excess mortality, the overuse of air-conditioning systems, the occurrence of wildfires in woodlands, cattle excess mortality, reduction in milk production, and variations in their enteric fermentation. The estimate of sub-risks has required the setting up of the hazard, exposure, and vulnerability maps. The hazard maps have been obtained through (8) by combining the daily magnitude M_d (Russo *et al* 2014, 2015) and the acclimatization index for excess heat EHI (accl) (Nairn and Fawcett 2015). Several vulnerability factors have been built through (2) to link the exposed elements with their predisposition to be affected or affect the environment during heatwaves. The sum of all the sub-risks provides a total heatwave risk equal to 2.55×10^6 € d^{-1} in the entire selected area. Despite the contribution of cattle milk reduction and woodland wildfires can be locally non-negligible, the major contributions in the current application result from air-conditioning systems (the 69%) and human excess mortality (the 28%), especially in the city of Bologna where most people live. Air conditioning is a helpful adaptation strategy to reduce heat stress but this strategy is not cost-effective and sustainable in the current world affected by anthropogenic climate change.

The application of the framework will be further expanded in future works to test explicitly the impacts of NbS. These works can benefit from previous studies that investigate how to refine heat maps (e.g. Zumwald *et al* 2021). Further improvements in the scientific literature would help to estimate the missing sub-risks and improve the estimated ones. Focusing on heatwaves, at least to our knowledge, current literature does not allow the estimate of reliable vulnerability factors that include temperature dependence for several sub-risks. Consequently, temperature affects only the H component leading to a linearization of sub-risks in which V is a fixed best

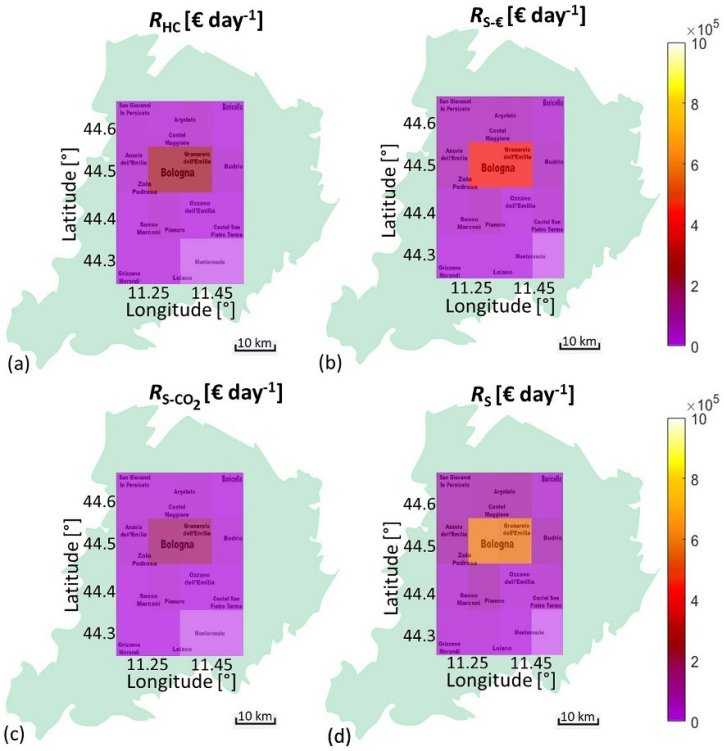

Figure 7. Healthcare risk resulting from excess mortality (a, $R_{HC-€}$), economic (b) and climate (c) contributions to the social sub-risk due to the usage of air-conditioning systems (i.e. $R_{S-€}$ and R_{S-CO_2}, respectively), and overall social sub-risk (d, R_S) for the study area in Bologna Province.

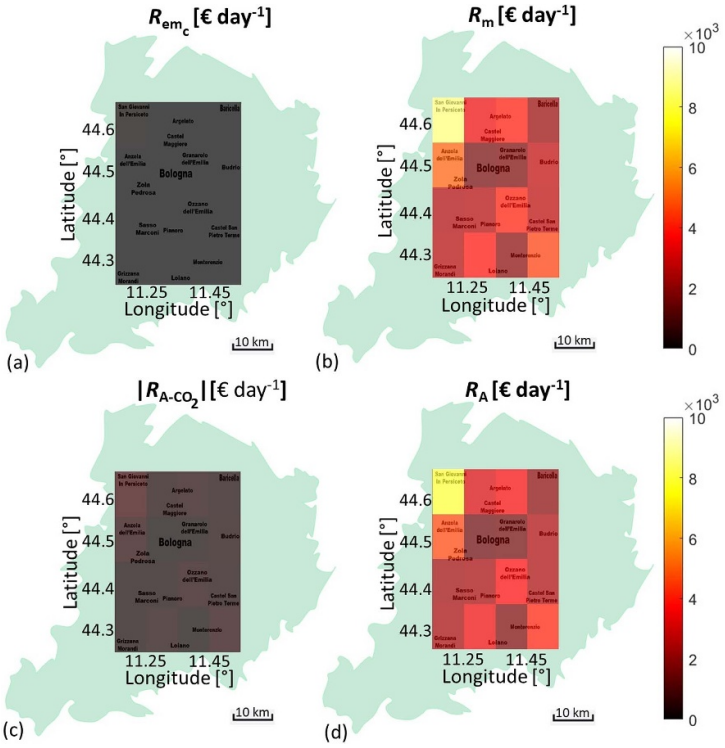

Figure 8. Economic ((a), cattle excess mortality R_{em_c}; (b), milk-production losses R_m), climate ((c), absolute value of enteric fermentation) contributions to the agricultural sub-risk (i.e. $R_{A-€}$ and R_{A-CO_2}, respectively), and overall agricultural sub-risk ((d), R_A) for the study area in Bologna Province.

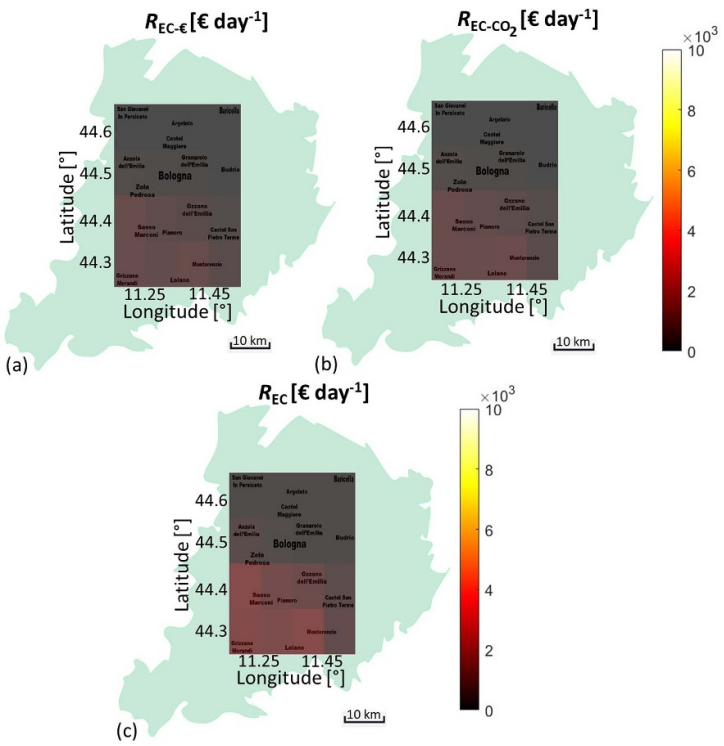

Figure 9. Economic (a), climate (b) contributions to the ecosystem sub-risk (i.e. $R_{EC-€}$ and R_{EC-CO_2}, respectively), and overall ecosystem sub-risk (c) due to woodland wildfires in the study area in Bologna Province.

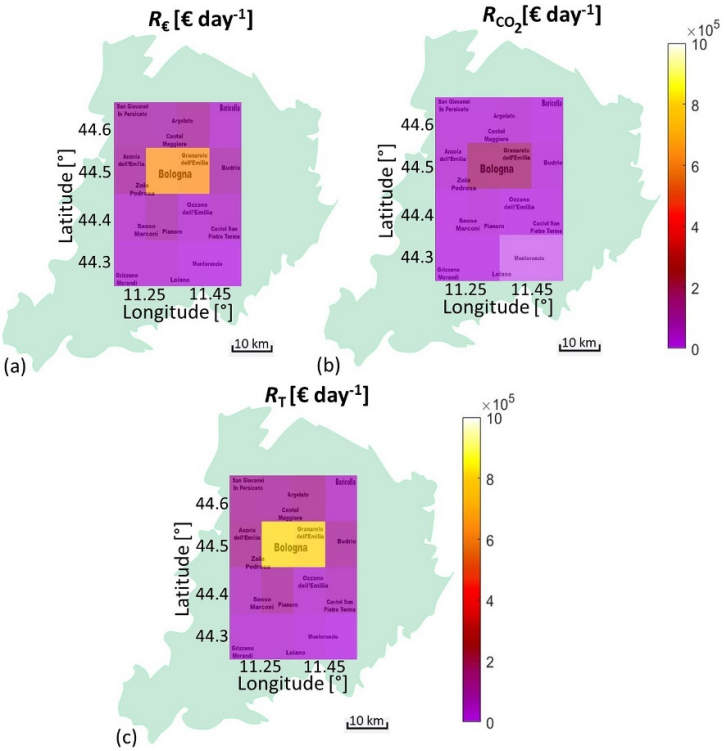

Figure 10. Economic (a, $R_€$), climate (b, R_{CO_2}), and total (c, R_T) risks for the study area in Bologna Province.

estimate obtained from the average of the impacts observed in previous events, and H acts as a temperature weight that considers both heatwave magnitude and living-being acclimatization. This approximation leads to the estimate of the average magnitude of risks. However, the combination of the framework with a sensitivity analysis or comprehensive uncertainty analysis (e.g. Kropf *et al* 2022) allows to expand

the output to a range of possible outcomes. This is particularly important in prognostic applications that investigate hazards H dominated by stochasticity. Another source of uncertainty is the existence of non-economic risks (e.g. the loss of aesthetic and spiritual ecosystem services; Renaud *et al* 2007) and vulnerability factors (e.g. lack of policies that support ecosystem robustness; Shah *et al* 2023) which are not covered by the framework. However, it is worth mentioning that non-economics co-benefits resulting from strategies (e.g. well-being and air quality; Ommer *et al* 2022) can be integrated into the framework by taking into account their economic impacts (e.g. the economic contribution to the healthcare sub-risk). The current paper wishes to encourage more studies concerning both sustainable strategies (e.g. NbS) and risk assessments that integrate a wider overall vision of the possible consequences resulting from hydro-meteorological hazards.

Data availability statement

All data that support the findings of this study are included within the article (and any supplementary files).

Acknowledgments

This research was founded by both the OPERANDUM and TRIGGER projects. These projects have received founding from the European Union under GA 776848; H2020 Programme and GA 101057739; Horizon Europe Health Programme, respectively.

ORCID iDs

L Brogno https://orcid.org/0000-0002-5920-8792
F Barbano https://orcid.org/0000-0002-4403-7070
L S Leo https://orcid.org/0000-0003-4103-6862
S Di Sabatino https://orcid.org/0000-0003-2716-9247

References

Adélaïde L, Chanel O and Pascal M 2022 Health effects from heat waves in France: an economic evaluation *Eur. J. Health Econ.* **23** 1–13

Alduchov O A and Eskridge R E 1996 Improved magnus form approximation of saturation vapor pressure *J. Appl. Meteorol. Climatol.* **35** 601–9

ARERA 2022 Cost of domestic electricity consumption, national regulatory authority for energy networks and environment (available at: www.arera.it/area-operatori/prezzi-e-tariffe) (Accessed 14 March 2023)

Aubrecht C and Özceylan D 2013 Identification of heat risk patterns in the US national capital region by integrating heat stress and related vulnerability *Environ. Int.* **56** 65–77

Berry I, Shanklin M and Johnson H 1964 Dairy shelter design based on milk production decline as affected by temperature and humidity *Trans. ASAE* **7** 329–0331

Buscail C, Upegui E and Viel J-F 2012 Mapping heatwave health risk at the community level for public health action *Int. J. Health Geograph.* **11** 1–9

CFPC 2019 Statistical analysis of forest fires 2017-2019 (Carabinieri - Forest Protection Command) (available at: www.carabinieri.it/docs/default-source/default-document-library/documento-analisi-incedi-triennio-2017-2019.pdf?sfvrsn=951f0723_0) (Accessed 5 March 2023)

CFPC 2021 Statistical analysis of forest fires 2021 (Carabinieri - Forest Protection Command) (available at: www.carabinieri.it/docs/default-source/carabinieri-forestali/analisi-statistica-incendi-boschivi-2021.pdf?sfvrsn=e68df223_2) (Accessed 14 March 2023)

CLAL 2022a Italy: milk production and use (CLAL) (available at: www.clal.it/index.php?section=bilancio_approv2&year=2022) (Accessed 23 Febuary 2023)

CLAL 2022b Reggio Emilia - price of milk for the production of parmigiano reggiano (CLAL) (available at: www.clal.it/?section=latte_reggio_emilia) (Accessed 23 Febuary 2023)

Cohen-Shacham E, Walters G, Janzen C and Maginnis S 2016 Nature-based solutions to address global societal challenges *IUCN: Gland, Switzerland* vol 97 pp 2016–36

Copernicus Climate Change Service, C. D. S. 2020 Fire danger indicators for Europe from 1970 to 2098 derived from climate projection (Copernicus Climate Change Service (C3S) Climate Data Store (CDS)) (Accessed 05 March 2023)

Copernicus Climate Change Service, C. D. S. 2022 European forest fire information system - seasonal trend for European Union (available at: https://effis.jrc.ec.europa.eu/apps/effis.statistics/seasonaltrend) (Accessed 05 March 2023)

Crichton D 1999 The risk triangle *Nat. Disaster Manage.* **102** 102–3

Curriero F C, Heiner K S, Samet J M, Zeger S L, Strug L and Patz J A 2002 Temperature and mortality in 11 cities of the eastern United States *Am. J. Epidemiol.* **155** 80–87

Debele S E *et al* 2023 Nature-based solutions can help reduce the impact of natural hazards: a global analysis of NBS case studies *Sci. Total Environ.* **902** 165824

Dubey A K, Lal P, Kumar P, Kumar A and Dvornikov A Y 2021 Present and future projections of heatwave hazard-risk over India: a regional earth system model assessment *Environ. Res.* **201** 111573

EER 2010 Cattle demography, number of animals per province and type of farming (Emilia-Romagna Region) (available at: https://sasweb.regione.emilia-romagna.it/statistica/Tabella.do?tabella=197) (Accessed 23 Febuary 2023)

ERR 2020 Detail land use vector covers (Emilia-Romagna Region) (available at: https://geoportale.regione.emilia-romagna.it/catalogo/dati-cartografici/pianificazione-e-catasto/uso-del-suolo/layer-9) (Accessed 15 Febuary 2023)

Feng D, Shi X and Renaud F G 2023 Risk assessment for hurricane-induced pluvial flooding in urban areas using a GIS-based multi-criteria approach: a case study of hurricane harvey in Houston, USA *Sci. Total Environ.* **904** 166891

Gasparrini A and Armstrong B 2011 The impact of heat waves on mortality *Epidemiology* **22** 68

Guarino M-V, Martilli A, Di Sabatino S and Leo L 2014 Modelling the urban boundary-layer over a typical mediterranean city using WRF: assessment of UHI and thermal comfort *Fluids Engineering Division Summer Meeting* vol 46247 (American Society of Mechanical Engineers) p V01DT28A006

GWIS 2023 Global wildfire information system (European Commission) (available at: https://gwis.jrc.ec.europa.eu/apps/gwis_current_situation/) (Accessed 5 March 2023)

Holec J, Sveda M, Szatmari D, Feranec J, Bobal'ova H, Kopecka M and St'astny P 2021 Heat risk assessment based on mobile phone data: case study of Bratislava, Slovakia *Nat. Hazards* **108** 3099–120

IHM 2022 Cattle demography, national zootechnical registry, Italian Health Ministry (available at: www.vetinfo.it/j6_statistiche/#/report-pbi/11) (Accessed 23 Febuary 2023)
IQFireWatch 2023 Global impacts of wildfires (available at: www.iq-firewatch.com/risk) (Accessed 5 March 2023)
IRDR 2014 Peril Classification and Hazard Glossary (IRDR DATA Publication No. 1) (Integrated Research on Disaster Risk)
ISMEA 2022 Cattle - prices for reimbursement of slaughtered animals (Italian Institute of Services for the Agricultural and Food Market) (available at: www.ismeamercati.it/flex/cm/pages/ServeBLOB.php/L/IT/IDPagina/12276) (Accessed 12 October 2023)
ISPRA 2023 Efficiency and decarbonization indicators in Italy and in the biggest European countries (Italian Institute for Environmental Protection and Research) (available at: www.isprambiente.gov.it/files2023/pubblicazioni/rapporti/r386-2023.pdf) (Accessed 06 November 2023)
ISTAT 2021 Energy consumption of households (Italian Institute of Statistics) (available at: www.istat.it/it/files/2022/06/REPORT-CONSUMI-ENERGETICI-FAMIGLIE-2021-DEF.pdf) (Accessed 14 March 2023)
ISTAT 2022a Crops: surfaces and production (Italian Institute of Statistics) (available at: http://dati.istat.it/Index.aspx?QueryId=37850) (Accessed 23 Febuary 2023)
ISTAT 2022b Resident population on 1st January (Italian Institute of Statistics) (available at: http://dati.istat.it/Index.aspx?QueryId=18560) (Accessed 18 Febuary 2023)
Johnson K, Depietri Y and Breil M 2016 Multi-hazard risk assessment of two Hong Kong districts *Int. J. Disaster Risk Reduct.* **19** 311–23
Kc B, Shepherd J, King A W and Johnson Gaither C 2021 Multi-hazard climate risk projections for the United States *Nat. Hazards* **105** 1963–76
Kikstra J S, Waidelich P, Rising J, Yumashev D, Hope C and Brierley C M 2021 The social cost of carbon dioxide under climate-economy feedbacks and temperature variability *Environ. Res. Lett.* **16** 094037
Kropf C M, Ciullo A, Otth L, Meiler S, Rana A, Schmid E, McCaughey J W and Bresch D N 2022 Uncertainty and sensitivity analysis for probabilistic weather and climate-risk modelling: an implementation in CLIMADA v. 3.1. 0 *Geosci. Model Dev.* **15** 7177–201
Lallo C H, Cohen J, Rankine D, Taylor M, Cambell J and Stephenson T 2018 Characterizing heat stress on livestock using the temperature humidity index (THI)-prospects for a warmer caribbean *Reg. Environ. Change* **18** 2329–40
Lee S-h, Kang J E, Park C S, Yoon D and Yoon S 2020 Multi-risk assessment of heat waves under intensifying climate change using bayesian networks *Int. J. Disaster Risk Reduct.* **50** 101704
Lüthi S *et al* 2023 Rapid increase in the risk of heat-related mortality *Nat. Commun.* **14** 4894
Masson-Delmotte V *et al* 2021 Climate change 2021: the physical science basis *Contribution of Working Group I to the Sixth Assessment Report of the Intergovernmental Panel on Climate Change (IPCC)* vol 2
Muñoz Sabater J 2019 Era5-land hourly data from 1950 to present (Copernicus Climate Change Service (C3S) Climate Data Store (CDS)) (Accessed 10 Febuary 2023)
Nairn J R and Fawcett R J 2015 The excess heat factor: a metric for heatwave intensity and its use in classifying heatwave severity *Int. J. Environ. Res. Public Health* **12** 227–53
Nunes B, Paixão E, Dias C M, Nogueira P and Falcào J M 2011 Air conditioning and intrahospital mortality during the 2003 heatwave in Portugal: evidence of a protective effect *Occup. Environ. Med.* **68** 218–23
OECD 2019 Mortality, morbidity and welfare cost from exposure to environment-related risks, Economic Co-operation and Development (available at: https://stats.oecd.org/Index.aspx?DataSetCode=EXP_MORSC) (Accessed 18 Febuary 2023)
Ommer J, Bucchignani E, Leo L S, Kalas M, Vranić S, Debele S, Kumar P, Cloke H L and Di Sabatino S 2022 Quantifying co-benefits and disbenefits of nature-based solutions targeting disaster risk reduction *Int. J. Disaster Risk Reduct.* **75** 102966
Pörtner H O *et al* 2022 Climate change 2022: impacts, adaptation and vulnerability *Contribution of Working Group II to the Sixth Assessment Report of the Intergovernmental Panel on Climate Change (IPCC)*
Renaud F G, Bogardi J J, Dun O and Warner K 2007 *Control, Adapt or Flee: How to Face Environmental Migration?* (UNU-EHS)
Russo S, Dosio A, Graversen R G, Sillmann J, Carrao H, Dunbar M B, Singleton A, Montagna P, Barbola P and Vogt J V 2014 Magnitude of extreme heat waves in present climate and their projection in a warming world *J. Geophys. Res.: Atmos.* **119** 12–500
Russo S, Sillmann J and Fischer E M 2015 Top ten European heatwaves since 1950 and their occurrence in the coming decades *Environ. Res. Lett.* **10** 124003
Russo S, Sillmann J, Sippel S, Barcikowska M J, Ghisetti C, Smid M and O'Neill B 2019 Half a degree and rapid socioeconomic development matter for heatwave risk *Nat. Commun.* **10** 136
Sahani J, Kumar P, Debele S, Spyrou C, Loupis M, Aragao L, Porcù F, Shah M A R and Di Sabatino S 2019 Hydro-meteorological risk assessment methods and management by nature-based solutions *Sci. Total Environ.* **696** 133936
Shah M A R *et al* 2020 A review of hydro-meteorological hazard, vulnerability and risk assessment frameworks and indicators in the context of nature-based solutions *Int. J. Disaster Risk Reduct.* **50** 101728
Shah M A R *et al* 2023 Quantifying the effects of nature-based solutions in reducing risks from hydrometeorological hazards: examples from Europe *Int. J. Disaster Risk Reduct.* **93** 103771
Stalhandske Z, Nesa V, Zumwald M, Ragettli M S, Galimshina A, Holthausen N, Röösli M and Bresch D N 2021 Projected impact of heat on mortality and labour productivity under climate change in Switzerland *Nat. Hazards Earth Syst. Sci. Discuss.* **2021** 1–20
Taylor J, Wilkinson P, Davies M, Armstrong B, Chalabi Z, Mavrogianni A, Symonds P, Oikonomou E and Bohnenstengel S I 2015 Mapping the effects of urban heat island, housing and age on excess heat-related mortality in London *Urban Clim.* **14** 517–28
Tomlinson C J, Chapman L, Thornes J E and Baker C J 2011 Including the urban heat island in spatial heat health risk assessment strategies: a case study for Birmingham, UK *Int. J. Health Geograph.* **10** 1–14
UNDRR 2017 The disaster risk reduction (DRR) glossary (United Nations Office for Disaster Risk Reduction) (available at: www.undrr.org/drr-glossary/terminology) (Accessed 10 Febuary 2023)
Van Wagner C and Pickett T 1985 *Equations and Fortran Program for the Canadian Forest Fire Weather Index System* vol 33 (Canadian Forestry Service, Petawawa National Forestry Institute)
Vitali A, Felici A, Esposito S, Bernabucci U, Bertocchi L, Maresca C, Nardone A and Lacetera N 2015 The effect of heat waves on dairy cow mortality *J. Dairy Sci.* **98** 4572–9
Wei W, Shi S, Zhang X, Zhou L, Xie B, Zhou J and Li C 2020 Regional-scale assessment of environmental vulnerability in an arid inland basin *Ecol. Indicators* **109** 105792
X-Rates 2023 Monthly average exchange rate between dollars and euros (available at: www.x-rates.com/average/?from=USD&to=EUR&amount=1&year=2022) (Accessed 20 October 2023)
Yadav B, Singh G, Wankar A, Dutta N, Chaturvedi V and Verma M R 2016 Effect of simulated heat stress on digestibility, methane emission and metabolic adaptability in crossbred cattle *Asian Australas. J. Animal Sci.* **29** 1585

Yin C, Yang F, Wang J and Ye Y 2020 Spatiotemporal distribution and risk assessment of heat waves based on apparent temperature in the one belt and one road region *Remote Sens.* **12** 1174

Zemtsov S, Shartova N, Varentsov M, Konstantinov P, Kidyaeva V, Shchur A, Timonin S and Grischchenko M 2020 Intraurban social risk and mortality patterns during extreme heat events: a case study of Moscow, 2010-2017 *Health Place* **66** 102429

Zumwald M, Knüsel B, Bresch D N and Knutti R 2021 Mapping urban temperature using crowd-sensing data and machine learning *Urban Clim.* **35** 100739